Accelerated Publications

Structural Basis for the Catalytic Mechanism of a Proficient Enzyme: Orotidine 5′-Monophosphate Decarboxylase[†,‡]

Pernille Harris,[§] Jens-Christian Navarro Poulsen,[§] Kaj Frank Jensen,[||] and Sine Larsen*[,§]

Centre for Crystallographic Studies, University of Copenhagen, Universitetsparken 5, 2100 Copenhagen, Denmark, and Institute of Molecular Biology, University of Copenhagen, Sølvgade 83H, B07 Copenhagen, Denmark

Received December 27, 1999; Revised Manuscript Received February 7, 2000

ABSTRACT: Orotidine 5′-monophosphate decarboxylase (ODCase) catalyzes the decarboxylation of orotidine 5′-monophosphate, the last step in the *de novo* synthesis of uridine 5′-monophosphate. ODCase is a very proficient enzyme [Radzicka, A., and Wolfenden, R. (1995) *Science 267*, 90−93], enhancing the reaction rate by a factor of 10^{17}. This proficiency has been enigmatic, since it is achieved without metal ions or cofactors. Here we present a 2.5 Å resolution structure of ODCase complexed with the inhibitor 1-(5′-phospho-β-D-ribofuranosyl)barbituric acid. It shows a closely packed dimer composed of two α/β-barrels with two shared active sites. The orientation of the orotate moiety of the substrate is unambiguously deduced from the structure, and previously proposed catalytic mechanisms involving protonation of O2 or O4 can be ruled out. The proximity of the OMP carboxylate group with Asp71 appears to be instrumental for the decarboxylation of OMP, either through charge repulsion or through the formation of a very short O···H···O hydrogen bond between the two carboxylate groups.

Orotidine 5′-monophosphate decarboxylase (ODCase)[1] catalyzes the decarboxylation of orotidine 5′-monophosphate (OMP) to uridine 5′-monophosphate (UMP). The reaction shown in Figure 1 is the last step in the *de novo* biosynthesis of UMP. In bacteria and fungi, ODCase is a monofunctional enzyme, while in mammals, it is the C-terminal part of the bifunctional UMP synthase. The N-terminal part of UMP synthase, equivalent to orotate phosphoribosyltransferase (OPRTase) in bacteria and fungi (*2*), catalyzes the fifth step in the *de novo* synthesis of UMP. The structure of OPRTase has been known for some time (*3*, *4*), and the catalytic mechanism of this enzyme has been thoroughly investigated (*5*).

ODCase is one of the most proficient enzymes. At ambient temperatures, it enhances the rate of reaction by a factor of 10^{17} (*1*). Considering the extreme proficiency the mechanism of ODCase is unique, because no cofactor is required for the decarboxylation. A covalent mechanism involving binding of a nucleophilic enzyme residue to C5 of the substrate,

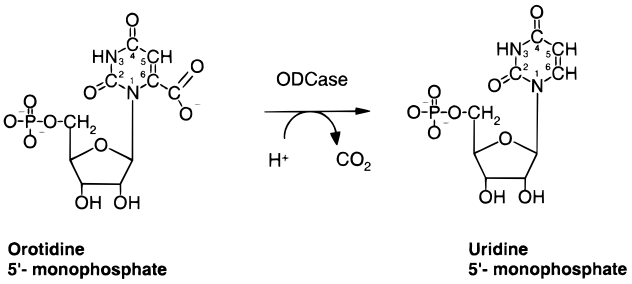

FIGURE 1: Schematic representation of the overall reaction catalyzed by ODCase.

followed by elimination of the carboxylate group, was suggested (*6*). This mechanism was not supported by ^{13}C NMR studies which established that C5 does not change from sp^2 hybridization to sp^3 hybridization during the reaction (*7*, *8*). The mechanism most likely being employed in neutral solvent has appeared to be the one suggested by Beak and Siegel (*9*). This involves an enzyme residue which protonates the C2 ketonic oxygen, O2, to form a nitrogen ylide intermediate, which acts as an electronic sink (a zwitterion). The charge distribution then helps to eliminate the carboxylate group. Recently, quantum mechanical calculations by Lee and Houk (*10*) made these authors suggest that a weak acid donates a proton to O4 of the substrate, thereby stabilizing another zwitterion in resonance with a neutral carbene.

Extensive enzymological studies have been performed on the yeast ODCase. Smiley and Jones (*11*) have shown that Lys93 in the yeast enzyme is critical for catalysis of the substrate to product, as well as for the binding of inhibitors.

† This work has been supported by the Danish National Research Foundation.

‡ Coordinates and structure factors have been deposited in the Protein Data Bank. The access code is 1EIX.

* To whom correspondence should be addressed. E-mail: sine@ccs.ki.ku.dk. Fax: +45 35320299. Telephone: +45 35320282.

§ Centre for Crystallographic Studies, University of Copenhagen.

|| Institute of Molecular Biology, University of Copenhagen.

[1] Abbreviations: ODCase, orotidine 5′-monophosphate decarboxylase; OPRTase, orotate phosphoribosyltransferase; UMP, uridine 5′-monophosphate; OMP, orotidine 5′-monophosphate; BMP, 1-(5′-phospho-β-D-ribofuranosyl)barbituric acid; NCS, noncrystallographic symmmetry; k_{cat}, turnover number; K_m, Michaelis constant; K_I, dissociation constant for the enzyme−inhibitor complex; k_{non}, noncatalytic rate constant; $\Delta\Delta G^{\ddagger}$, difference in the activation free energy.

10.1021/bi992952r CCC: $19.00
Published on Web 03/23/2000

Table 1: Data Collection and Processing

	ODCase−BMP	Se-Met-ODCase−BMP
X-ray source	beamline 7-11, MAXLAB, Lund, Sweden	BM14 ESRF, Grenoble, France
detector	Mar research image plate	Mar research CCD
wavelength (Å)	0.9902	0.9787 (pk), 0.9789 (ip), 0.8856 (rm)
temperature (K)	99.9	105
space group	$P2_12_12_1$	$P2_12_12_1$ (pseudo)
cell parameters (Å)	$a = 61.30(7)$	$a = 61.82(1)$
	$b = 95.99(23)$	$b = 97.68(21)$
	$c = 145.08(19)$	$c = 148.89(26)$
resolution[a] (Å)	30.0−2.5 (2.64−2.50)	30.0−3.0 (3.16−3.00)
no. of total reflections	102335	55386 (pk), 55237 (ip), 55577 (rm)
no. of unique reflections	29678	18413 (pk), 18400 (ip), 18346 (rm)
completeness	98.0 (92.4)	98.6 (89.1) (pk), 98.6 (90.3) (ip), 98.4 (90.0) (rm)
$I/\sigma(I)$	10.6 (5.2)	8.9 (3.9) (pk), 8.6 (3.4) (ip), 9.2 (4.1) (rm)
R_{merge}	0.088	0.108 (pk), 0.114 (ip), 0.104 (rm)

[a] The numbers in parentheses refer to the outermost resolution shell.

The K93C mutant protein recovers some activity after treatment with bromoethylamine, showing that the amino group of Lys93 is essential for catalysis. No attempts have been made to reveal the role of other conserved amino acid residues in the ODCases.

Bell and Jones (*12*) have shown that at low concentrations, yeast ODCase is a monomer (if no phosphate or other ligands are added). ODCase is a dimer at higher enzyme concentrations and in the presence of nucleotides. The tightly bound inhibitor 1-(5′-phospho-β-D-ribofuranosyl)barbituric acid (BMP) has a K_i of 8.8×10^{-12} M at pH 6.0 (*13*), and also, 6-aza-UMP with a K_i of 0.51 μM at pH 6.0 inhibits ODCase. The product, UMP, binds to ODCase with a K_i of 0.46 mM at pH 6.0. Interestingly, the K93C mutant enzyme has a higher affinity for UMP than for 6-aza-UMP (*11*).

To gain an understanding of the mechanism of the enzyme, we have determined the three-dimensional structure of ODCase from *Escherichia coli* cocrystallized with the inhibitor BMP. Investigations of the *E. coli* enzyme show that the turnover number, k_{cat}, is essentially constant above pH 7 ($28\ s^{-1}$), but declines below pH 7. Its catalytic efficiency, k_{cat}/K_m, shows a sharp optimum around pH 7 very similar to that seen for the yeast enzyme (*14*). The Michaelis constant is minimal near pH 7, approximately 1 μM, and increases to either side of this pH value. UMP is a weak inhibitor of the reaction with a K_i of about 0.5 mM. The inhibition by BMP has been investigated at pH 8 in the presence of 100 μM OMP as a substrate. Even at a quite high dilution, the enzyme is inactivated (slowly) by stoichiometric concentrations of BMP, indicating a K_i for BMP of $\ll 10^{-8}$ M. Our conclusion is that *E. coli* ODCase displays activity, a pH optimum, and inhibition toward BMP similar to those of the yeast enzyme (*15*).

The result from a sequence alignment of 53 ODCases with a broad phylogenetic background, available from the SWISS-PROT database, is shown in Figure 2. This reveals five totally conserved amino acid residues corresponding to Lys44, Asp71, Lys73, Asp76, and Ile77 in the *E. coli* sequence. In addition, three amino acids (*E. coli*, Asp22, Thr80, and Arg222) are conserved in all but one sequence. The degree of identity between the *E. coli* and the yeast enzyme is 24%, and the degree of homology is 45%. Also, from the sequence alignment, we notice that the Lys93 residue in the yeast enzyme corresponds to Lys73 in the *E. coli* enzyme.

MATERIALS AND METHODS

ODCase from *E. coli* was expressed and purified from the *E. coli* strain NF 1830 that was transformed with the plasmid pLFF8, which carries the *E. coli pyr F* gene (*15*). The selenomethionine-substituted ODCase was expressed in *E. coli* strain SØ 6733, a derivative of *E. coli* strain DL41. The selenomethionine-substituted ODCase was purified as the native ODCase, except that a heat denaturation purification step was omitted. The same specific activity was observed for the selenomethionine-substituted ODCase and the native ODCase.

The ODCase−BMP complex was crystallized in hanging drops at 17 °C in 28% PEG 8000, 0.2 M $MgCl_2$, and 0.1 M MES (pH 7.0). The crystals were mounted using as cryoprotectant 20% glycerol included in the mother liquor. Data collection for the native ODCase−BMP crystals was performed at beamline BL7-11 at MAXLAB. The crystals diffracted to 2.5 Å. The selenomethionine-substituted ODCase−BMP complex was crystallized under similar conditions, in hanging drops at 17 °C in 20% PEG 8000, 0.2 M $MgCl_2$, and 0.1 M MES (pH 7.0). MAD data collection on the selenomethionine-substituted crystals was performed at beamline BM14 at the ESRF. These crystals diffracted to 3.0 Å. The absorption edge from the selenium atoms was checked by the X-ray fluorescence signal and was of a very high quality with a minimum f' of −10.4 electrons and a maximum f'' of 6.44 electrons. A summary of the data collections and successive data processing is shown in Table 1. A cell doubling of the unit cell of the selenomethionine-substituted crystal form was observed as compared to the crystals of the native protein. The cell doubling was seen as the appearance of rather weak diffraction spots between the diffraction spots that could be indexed in the unit cell and space group from the crystal form of the native protein complex.

The crystals of the native ODCase−BMP complex can be indexed in space group $P2_12_12_1$ with the following unit cell dimensions: $a = 61.3$ Å, $b = 96.0$ Å, and $c = 145.1$ Å. The crystals of the selenomethionine-substituted ODCase−BMP complex can be indexed in space group $C222_1$ ($a = 123.2$ Å, $b = 195.2$ Å, and $c = 148.9$ Å) or in space group $P2_1$ ($a = 115.5$ Å, $b = 149.0$ Å, $c = 115.6$ Å, and $\beta = 115.32°$). By looking at the merging statistics, we have determined the latter ($P2_1$) of these to be correct.

The data were processed in DENZO (*16*) and scaled in SCALA (*17*). The positions of the selenium atoms were determined using the program SOLVE (*18*). The weak reflections that were only seen in the selenomethionine-substituted crystal form were ignored, and only reflections corresponding to the smaller unit cell of the native crystal form were included, hence assuming space group $P2_12_12_1$. SOLVE was able to localize 24 of the 32 expected selenium

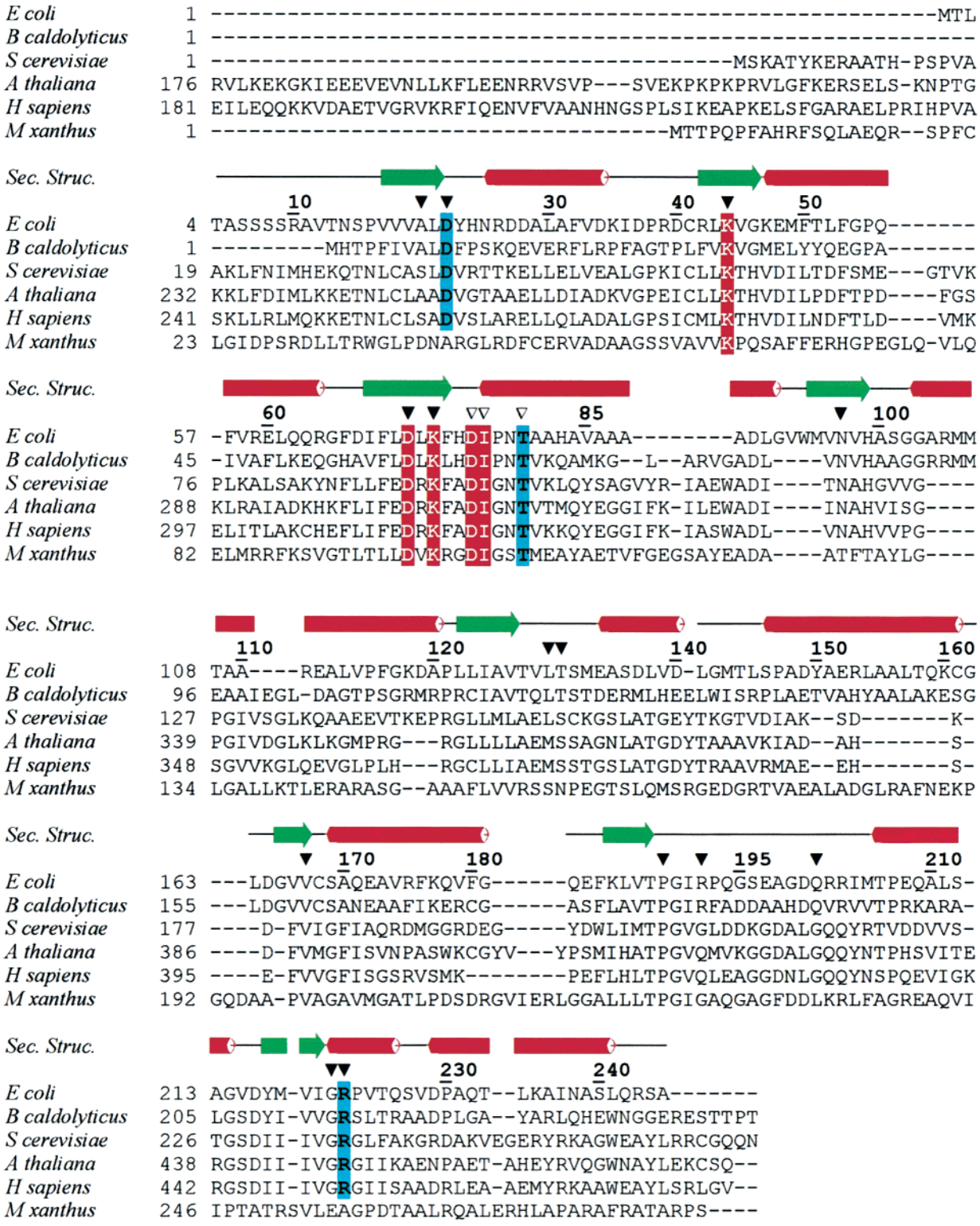

FIGURE 2: Alignment of 6 sequences of ODCases, based on the alignment of 53 ODCase sequences. Red shaded amino acids are conserved in all 53 sequences; blue shaded amino acids are conserved in 52 sequences. The amino acids marked with triangles are in the vicinity of the binding site of BMP. Amino acids marked with black triangles come from one subunit, while amino acids marked with white triangles come from the other subunit. Above the sequence the secondary structural elements are shown, identified in ODCase from *E. coli*.

atoms in the asymmetric unit. The noncrystallographic symmetry between the four subunits (two dimers) was found manually, and the maps were averaged using the CCP4 program DM (*17*). From this map, about two-thirds of the structure was built in TURBO (*19*). After a few cycles of simulated annealing using CNS (*20*), we were able to refine the structure to the native data set, hereby overcoming the problem of pseudosymmetry and obtaining a final structure resolution of 2.5 Å. The NCS-averaged electron density from these data was very clear, and the rest of the structure was easily built. Residues 12−242 are included in the model, indicating that the N-terminus and the last few residues of the C-terminus are disordered. The final refinement statistics are shown in Table 2.

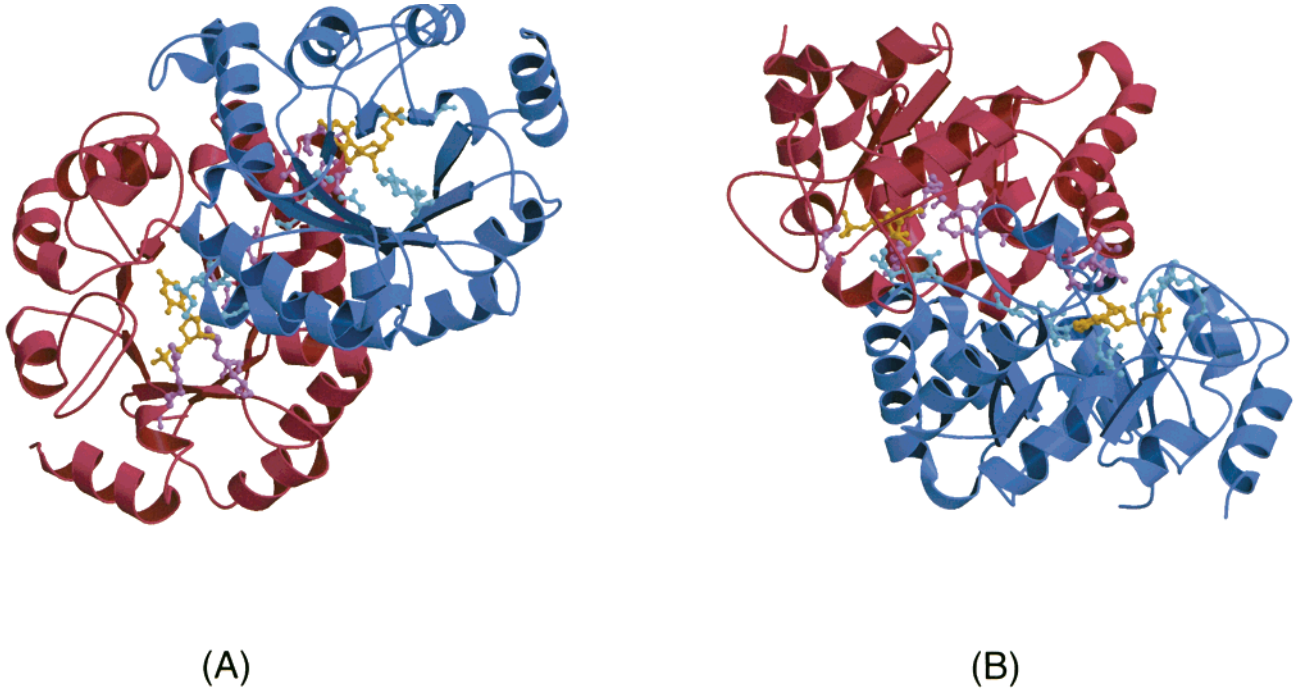

FIGURE 3: Homodimer of *E. coli* ODCase. One subunit is colored red and the other blue. Completely conserved residues are emphasized with ball-and-stick representations. The inhibitor, BMP, is drawn in yellow. (A) Viewed through the α/β-barrel. (B) Viewed perpendicular to the view in panel A. The figures were drawn using the programs MOLSCRIPT (*28*) and Raster3D (*29*). The two subunits are connected by a series of hydrogen bonds between residues His24 and Asp90; Lys73 and Asp76; N79 and Asp200; Arg105 and Ser132, Asp137, and Asp200; His75 and Lys47 and His99; and Asp200 and N79.

Table 2: Refinement Statistics

resolution range (Å)	30−2.5
no. of reflections	28179
no. of atoms	
protein	7000
ligand	88
water	415
rmsd (bond lengths) (Å)	0.007
rmsd (bond angles) (deg)	1.279
R	0.217
R_{free}	0.261

RESULTS

The asymmetric unit of the native protein contains four subunits arranged as two dimers where the two subunits are related by a 2-fold symmetry. Only amino acid residues involved in crystal contacts deviate from the noncrystallographic symmetry restraints enforced throughout the refinements. Each subunit folds up as an α/β-barrel where the eight central β-strands are surrounded by eleven helical segments (Figure 3). The homodimer of the ODCase−BMP complex is very closely packed with a BMP molecule in the C-terminal end of each barrel. Figure 3 shows that the residues that surround each inhibitor come from both subunits, so the two active sites are effectively shared by the two subunits. The separation between the active sites in the dimer is approximately 16 Å, measured as the distance between the Nϵ atoms of the catalytically important Lys73 residues.

Both BMP molecules in the dimer are completely embedded in the protein linked by an extensive set of hydrogen bonds to the surrounding protein as shown in Figure 4. Though the predominant interactions are with one subunit, BMP is also hydrogen bonded to the side chains of two conserved residues from the other subunit, Asp76B and Thr80B. This explains why dimer formation is favored by the addition of nucleotides. The two negative charges of the 5′-phosphate group are partly neutralized by the short hydrogen bonds to the positively charged residues Arg192 (2.4 Å) and Arg222 (2.6 Å). The interactions between Arg222 and BMP involve not only the side chain of Arg222 but also its backbone amide group. In addition, the phosphate group is hydrogen bonded to the backbone of Gly221. The ribose ring of BMP is tied to the active site by interactions with the two conserved residues, Lys44 and Asp22, both hydrogen bonded to the 3′-hydroxyl group. The 2′-hydroxyl group donates a proton to Asp76 and accepts a proton from Thr80, where both are conserved side chains from the neighboring subunit. The orientation of the pyrimidine ring with respect to Lys73, known to be important for catalysis, has been an important issue in the different models proposed for the catalytic function of the ODCases. The hydrophilic side, comprised of O4, N3, and O2, is engaged in hydrogen bonds to Thr131 and Gln201. The backbone NH group of Thr131 donates a proton to O4; its side chain OH group is an acceptor of a hydrogen bond from N3 and a donor to the CO group in the side chain of Gln201. The weak interactions with O4 could explain why the substrate analogue, 4-thio-OMP, is partially active (*8*). C5 at the opposite side of the pyrimidine ring does not have any close contacts with the surrounding protein. The C5-H group is pointing into a hydrophobic pocket.

DISCUSSION

The structural results allow us to evaluate the different catalytic mechanisms suggested for the ODCases. From the hydrogen bonding pattern of the BMP moiety, we notice that O4 is hydrogen bonded to the backbone N of the noncon-

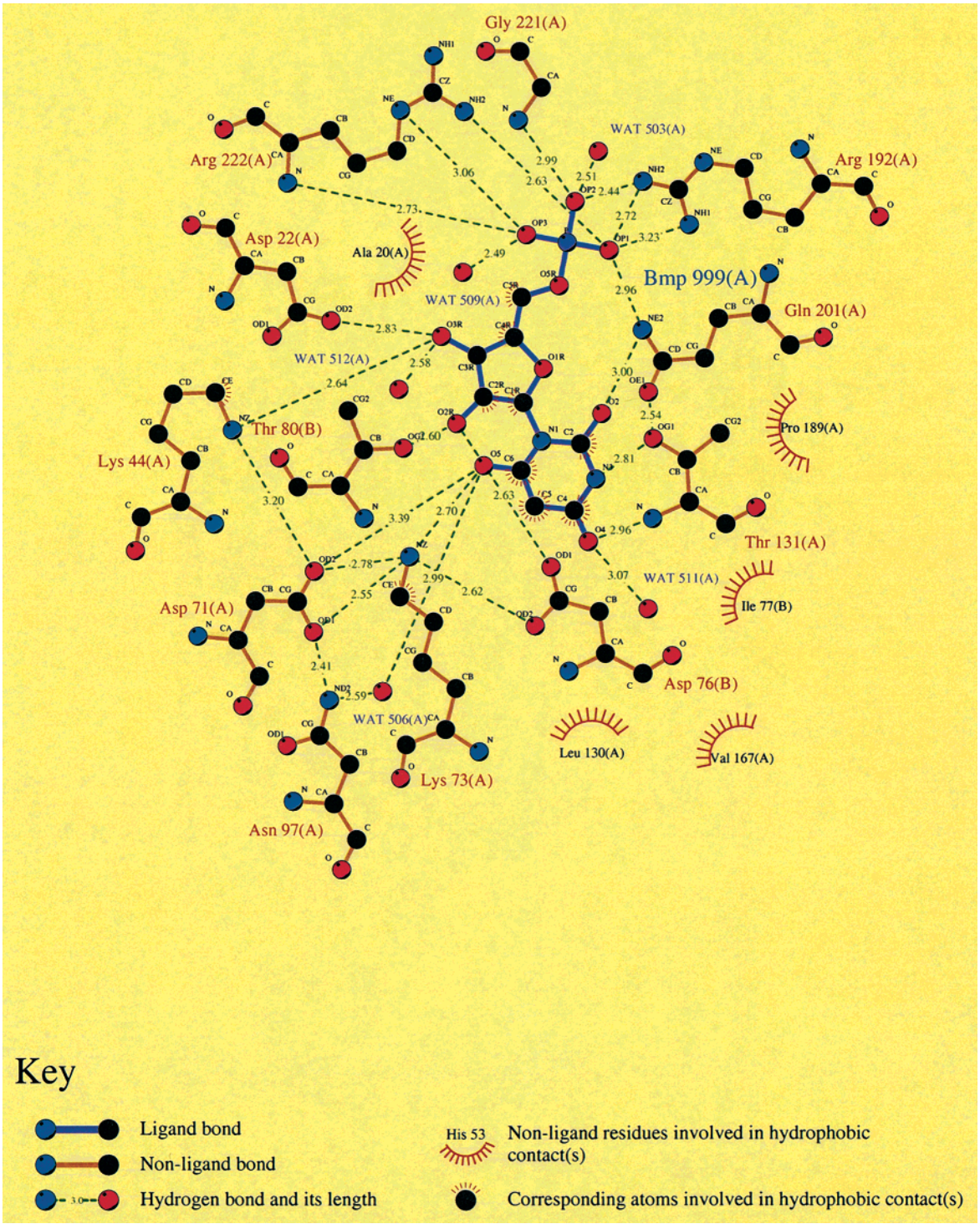

FIGURE 4: LIGPLOT (*30*) diagram of the hydrogen bonding pattern, and the hydrophobic interactions around the inhibitor, BMP.

served Thr131 with no other proton donor in the vicinity. A proton transfer to O4 of the orotate moiety as proposed from theoretical calculations (*10*) can, therefore, be ruled out.

The mechanism, where O2 in the orotate moiety is protonated before decarboxylation, is unlikely if we assume that OMP binds in the same (*syn*) conformation as we observe for BMP (based on the surroundings on N3 and C5). Here, O2 is hydrogen bonded to Nϵ2 of Gln201. To examine if the pyrimidine ring of OMP may be bound in the *anti* conformation, we tried to dock a CO_2^- group into what we believe is the wrong position. This would lead to considerable steric hindrance between the CO_2^- group and Cδ1 of the completely conserved residue Ile77B. The distance between the closest oxygen and Cδ1 of Ile77B would be approximately 2.4 Å. The three observations, *i.e.*, the hydrogen bonding possibility for N3, the hydrophobic environment of C5, and the steric hindrance of the CO_2^- group if OMP is in the *anti* configuration, are very important. They all support the *syn* configuration of OMP, and therefore, the enzymatic attack must be directly on C6 and the carboxylate group.

An inspection of the active site and the environment of BMP reveals some remarkable features. BMP is deeply buried in the protein with the pyrimidine ring covered by a series of hydrophobic residues: Ile77B, Val127A, Leu130A,

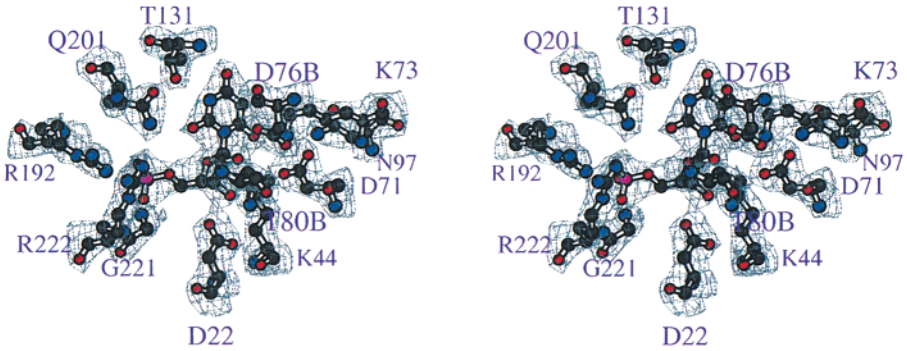

FIGURE 5: Stereoview of the active site around the inhibitor, BMP. The contour shows the SIGMAA-weighted $2F_o - F_c$ map contoured at 1.5σ. The programs O (*31*) and Molscript (*28*) were used to make the figure.

Val167A, Val187A, and Val219A.

Residues 190−205 form a loop shielding the active site. Two side chains from this loop (Arg192 and Gln201) are engaged in hydrogen bonds to the inhibitor. The active site contains a unique arrangement of totally conserved positively (Lys44 and Lys73) and negatively (Asp71 and Asp76) charged side chains as shown in Figure 5. Lys73, proven to play a role in catalysis, is linked to Asp71 and Asp76 by an almost symmetrical arrangement of hydrogen bonds. Asp71 has the two positively charged side chains of Lys73 and Lys44 in its immediate environment. The ODCase−BMP complex shows only direct hydrogen bonds between Asp71 and Lys73, but only a small conformational change of the side chain of Lys44 is required for it to make the hydrogen bond to Asp71. Such a hydrogen bond is observed in the structure of the apoenzyme (*21*) with Lys44 and Lys73 placed almost symmetrically on each side of Asp71. Replacing the pyrimidine moiety of BMP with an orotate ion in the same geometry as observed in the product complex of dihydroorotate dehydrogenase (*22*), we note that Oδ2 of Asp71 and a carboxy oxygen of the modeled OMP substrate are separated by ≈2.4 Å.

The close proximity of the two carboxylate groups makes us suggest two slightly different catalytic mechanisms. The first one, shown in Figure 6, is based on charge repulsion between the two negatively charged carboxylate groups of OMP and Asp71. The second suggestion, shown in Figure 7, is based on the formation of a very short, hydrogen bond between these two carboxylate groups.

Without the substrate or substrate analogues bound in the enzyme, the loop covering the active site comprised by residues 190−205 is in an open conformation (*21*). The first step in the reactions shown in Figures 6 and 7 involves closing of the loop and proper binding of the substrate (Figures 6A and 7A). The array, Lys44−Asp71−Lys73−Asp76, is uncharged in total, and this net charge of zero is possibly important for the acceptance of the negatively charged carboxylate part of OMP.

In the charge repulsion mechanism, Lys44 is turned away from Asp71 to bind to the ribose moiety and the negatively charged carboxylate group is now facing the negatively charged Asp71. This is energetically very unfavorable, and a possibility is that charge repulsion between these two groups will initiate decarboxylation as shown in Figure 6B. Nϵ from Lys73 and C6 of OMP are very close (3.5 Å), and Lys73 may easily be relaxed to be able to transfer a proton to C6. As UMP and CO_2 leave the active site (Figure 6C), a proton may be transferred from the solvent to the otherwise deprotonated Lys73 (Figure 6D).

In the second suggested mechanism, we note that when we replace the pyrimidine ring of BMP with orotate, the carboxylate group of OMP is approximately 2.4 Å from the carboxylate oxygen atom of Asp71; this is the O−O distance in the very short, strong O···H···O hydrogen bonds. These very strong hydrogen bonds which have O−O distances in the range of 2.35−2.55 Å are typically formed between carboxylate and carboxylic acid groups with similar pK_a values. They have been shown to have covalent character with hydrogen bond energies of more than 100 kJ mol^{-1} (*23*−*25*). The position of Asp71 between the two positively charged Lys residues (44 and 73) observed in the apoenzyme will make it a much stronger acid, so it seems likely that it attains a pK_a value comparable to the pK_a value of the carboxylic acid group of OMP. Binding of the substrate as shown in Figure 7A will bring the carboxylate group of the substrate so close to the carboxylate group of Asp71 that they can form the very short O···H···O hydrogen bond (Figure 7B), a transition state that resembles the one that leads to direct decarboxylation of β-keto acids (*26*). The proton connecting the two carboxylate groups in the very short O···H···O hydrogen bond could come from Lys44 (as suggested in Figure 7B). As Lys44 is turned away from Asp71 to make a hydrogen bond to O3′ of the ribose ring (equivalent to the one seen in the ODCase−BMP complex), the pK_a value of Asp71 increases. Hence, the proton in the low-barrier hydrogen bond will be transferred to the less acidic Asp71. Simultaneously, Lys73 is in a suitable position to transfer a proton to C6 and OMP decarboxylates (Figure 7B). The last step in the reaction involves a transfer of the proton from Asp71 to the deprotonated Lys73 residue (see Figure 7C) and a proton transfer from the solvent to Lys44, if this latter is deprotonated (Figure 7D).

The two reaction mechanisms described above involve all the completely conserved residues among the ODCase sequences. They are important either for substrate binding or for catalysis. It is worth noting that the latter mechanism also accounts for one of the salient features of the ODCases, its very sharp pH optimum close to pH 7.0. The mechanism relies on the fine interplay of interactions between aspartic acid and lysine residues, whose side chains are titrated on either side of pH 7.

We want to stress that, except for the initial closing of the loop when the substrate binds, the two proposed mechanisms are based on the movement of protons and

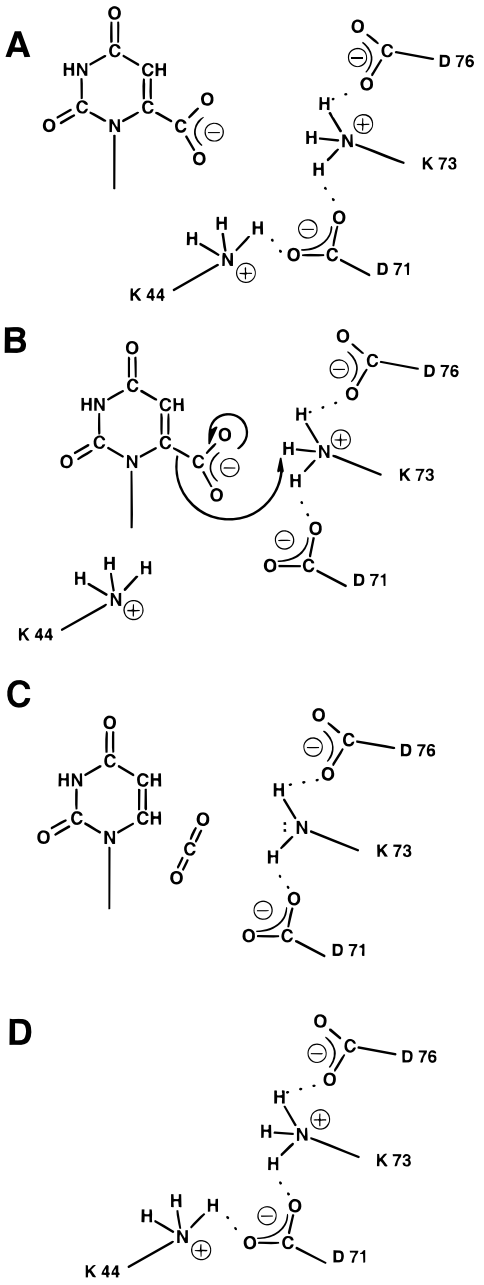

FIGURE 6: Stepwise representation of the first proposed mechanism used by ODCase in the decarboxylation of OMP. (A) The substrate enters the active site. (B) As Lys44 is turning away from Asp71, charge repulsion between the two carboxylate groups initiates decarboxylation and Lys73 donates a proton to C6. (C) CO_2 and UMP leave the active site. (D) Lys73 is protonated from the solvent.

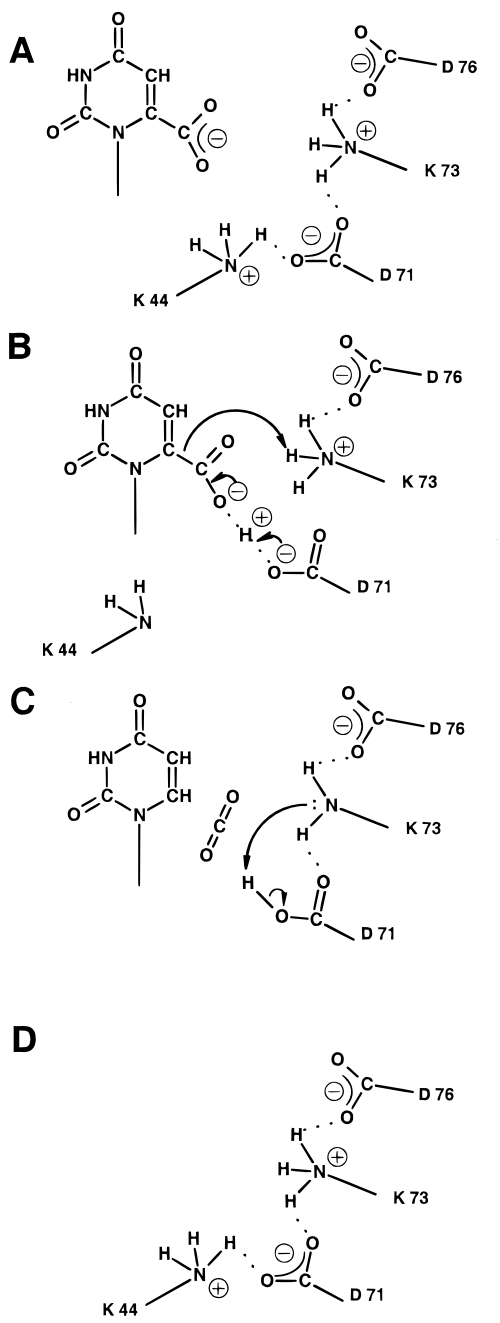

FIGURE 7: Stepwise representation of the second proposed mechanism used by ODCase in the decarboxylation of OMP. (A) The substrate enters the active site. (B) In the transition state, a very short hydrogen bond between Asp71 and the carboxylate group of OMP is formed and Lys44 turns toward the ribose moiety. As the pK_a for OMP is now the lower value, the proton is transferred to Asp71, and Lys73 donates a proton to C6. (C) The proton on Asp71 is transferred to Lys73. (D) The product has left the active site, and Lys44 is protonated from the solvent and returns to its original position.

electrons and partially achieved through small adjustments of Lys44 and Lys73. Also, the proposed mechanisms provide an explanation for the total conservation of residues Lys44, Asp71, Lys73, Asp76, and Ile77. Ile77 serves as a plug, assuring that the substrate binds in the *syn* conformation. Asp76 is taking part in the array of charged residues in the active site. It is hydrogen bonded to Lys73, and probably involved in the fine-tuning of the pH optimum and the correct position of Lys73. Lys44, Asp71, and Lys73 are directly involved in the mechanism. Lys44, initially being hydrogen bonded to Asp71, provides a positive charge so that the substrate binds, and also has the possibility of donating a proton to the suggested short low-barrier hydrogen bond between Asp71 and the substrate. Asp71 is initiating decarboxylation of OMP, and finally, Lys73 is providing the proton to C6.

The latter mechanism, involving the O···H···O short hydrogen bond, is in agreement with recent measurements of the D_2O solvent kinetic isotope effects and the ^{13}C primary kinetic isotope effects on *E. coli* ODCase (*27*), which show that decarboxylation and proton transfer occur in separate steps and that proton transfer must occur prior to decarboxylation.

The rate enhancement of ODCase, defined as k_{cat}/k_{non}, has been calculated to be 10^{17}. The corresponding estimate of the difference in the activation free energy, $\Delta\Delta G^{\ddagger}$, between the catalyzed and noncatalyzed reaction is accordingly $\approx RT \ln 10^{17}$, which at 300 K is ≈100 kJ. Here it should be noted that bringing two point charges of $^1/_2e^-$ together to a distance of only 2.3 Å will *cost* about 150 kJ, while the energy that may be *gained* by forming a short O···H···O hydrogen bond between a carboxylic acid and a carboxylate group is approximately 100 kJ.

To distinguish between the two proposed mechanisms, further experiments are required, for instance, on suitable mutant enzymes.

ACKNOWLEDGMENT

Lise Schack and Flemming Hansen are thanked for technical assistance, and Gordon Leonard at BM14, ESRF, is thanked for help with the MAD experiments. Johan G. Olsen, Per Ola Norrby, Jens Bukrinsky, and Martin Willemoës have been helpful with assistance and fruitful discussions about the mechanism.

REFERENCES

1. Radzicka, A., and Wolfenden, R. (1995) *Science 267*, 90−93.
2. Traut, T. W., and Jones, M. E. (1996) *Prog. Nucleic Acid Res. Mol. Biol. 53*, 1−78.
3. Scapin, G., Grubmeyer, C., and Sacchettini, J. C. (1994) *Biochemistry 33*, 1287−1294.
4. Henriksen, A., Aghajari, N., Jensen, K. F., and Gajhede, M. (1996) *Biochemistry 35*, 3803−3809.
5. Wang, G. P., Lundegaard, C., Jensen, K. F., and Grubmeyer, C. (1999) *Biochemistry 38*, 275−283.
6. Silverman, R. B., and Groziak, M. P. (1982) *J. Am. Chem. Soc. 104*, 6434.
7. Acheson, S. A., Bell, J. B., Jones, M. E., and Wolfenden, R. (1990) *Biochemistry 29*, 3198−3202.
8. Shostak, K., and Jones, M. E. (1992) *Biochemistry 31*, 12155−12161.
9. Beak, P., and Siegel, B. (1976) *J. Am. Chem. Soc. 98*, 3601−3606.
10. Lee, J. K., and Houk, K. N. (1997) *Science 276*, 942−945.
11. Smiley, J. A., and Jones, M. E. (1992) *Biochemistry 31*, 12162−12168.
12. Bell, J. B., and Jones, M. E. (1991) *J. Biol. Chem. 266*, 12662−12667.
13. Levine, H. L., Brody, R. S., and Westheimer, F. H. (1980) *Biochemistry 19*, 4993−4999.
14. Smiley, J. A., Paneth, P., O'Leary, M. H., Bell, J. B., and Jones, M. E. (1991) *Biochemistry 30*, 6216−6223.
15. Poulsen, J.-C. N., Harris, P., Jensen, K. F., and Larsen, S. (1999) Manuscript to be published.
16. Gerwith, D. (1999) *The HKL-manual: On oscillation Data Processing Suite for Macromolecular Crystallography*, Yale University, New Haven, CT.
17. The CCP4 Suite and Programs for Protein Crystallography (1994) *Acta Crystallogr. D 50*, 750−763.
18. Terwilliger, T. C., and Berendzen, J. (1999) *Acta Crystallogr. D 55*, 849−861.
19. Roussel, A., and Cambillau, C. (1992) *TURBO-FRODO biographics and AFMP. Architecture et Function des Macromolécules Biologique.*
20. Brünger, A. T., Adams, P. D., Clore, G. M., Delano, W. L., Gros, P., Grosse-Kunstlere, R. W., Jiang, J.-S., Kuszewski, J., Nilges, N., Pannu, N. S., Read, R. J., Rice, L. M., Simonson, T., and Warren, G. L. (1998) *Acta Crystallogr. D 54*, 905−921.
21. Harris, P., Poulsen, J.-C. N., Jensen, K. F., and Larsen, S. (1999) unpublished results.
22. Rowland, P., Bjornberg, O., Nielsen, F. S., Jensen, K. F., and Larsen, S. (1998) *Protein Sci. 7*, 1269−1279.
23. Flensburg, C., Stewart, R. F., and Larsen, S. (1995) *J. Phys. Chem. 99*, 1030−1041.
24. Madsen, D., Flensburg, C., and Larsen, S. (1998) *J. Phys. Chem. A 102*, 2177−2188.
25. Abu-Dari, K., Raymond, K. N., and Freyberg, D. P. (1979) *J. Am. Chem. Soc. 101*, 3639.
26. March, J. (1992) in *Advances in Organic Chemistry*, pp 628, Wiley, New York.
27. Erhlich, J. I., Hwang, C.-C., Cook, P. F., and Blanchard, J. S. (1999) *J. Am. Chem. Soc. 121*, 6966−6967.
28. Kraulis, P. J. (1991) *J. Appl. Crystallogr. 24*, 946−950.
29. Merrit, E. A., and Bacon, D. J. (1999) *Methods Enzymol. 277*, 505−524.
30. Wallace, A. C., Laskowski, R. A., and Thornton, J. M. (1995) *Protein Eng. 8*, 127−134.
31. Jones, T., Zou, J.-Y., Cowan, S., and Kjeldgaard, M. (1991) *Acta Crystallogr. D 50*, 110−119.

BI992952R